

Whistler Studies of the Plasmapause in the Magnetosphere

2. Electron Density and Total Tube Electron Content near the Knee in Magnetospheric Ionization

J. J. ANGERAMI¹ AND D. L. CARPENTER

Radioscience Laboratory, Stanford University, California

Abstract. A study has been made of electron density and total electron content in tubes of force near the knee in magnetospheric ionization. It was based on whistler observations made at Eights, Antarctica, in July and August 1963, under conditions of steady, moderate geomagnetic agitation ($K_p = 2-4$). During the period 0100-0400 LT, the electron density near the equatorial plane at a geocentric distance of $4 R_E$ drops a factor of 30-100 within a distance of less than $0.15 R_E$. The corresponding change in tube content above 1000 km is a factor of about 10 within less than a degree of latitude. The afternoon profiles are generally similar to the postmidnight results. In the afternoon the profiles are often well defined outside the knee, falling smoothly to about 1 el/cm³ at $7 R_E$. Both the equatorial and tube content profiles show a definite repeatability between observations at a given local time and under conditions of moderate, steady geomagnetic agitation. Diurnal effects are evident, with amplitude differing from point to point on the profiles. The problem of the field-line distribution of ionization has been studied with a view to minimizing error in the profiles. Experimental and theoretical support has been found for using a diffusive-equilibrium distribution along the field lines inside the knee and a 'collisionless' model, behaving approximately as $N_e \propto R^{-4}$, along the field lines outside the knee. A study of error shows that the uncertainty in individual points on the knee profiles is everywhere less than a factor of ± 2 , and on the content profiles less than a factor of ± 1.5 .

INTRODUCTION

The principal purpose of this paper is to describe details of electron density and total tube electron content near the knee in magnetospheric ionization. The results are drawn from the whistler data from which the companion paper, K-1 [Carpenter, 1966], was prepared. A part of this report will be devoted to discussion of the field-line electron-density models used in the calculations and to error in the experimental results.

Introductory material on the knee phenomenon and on the whistler experiment was presented in K-1, and we therefore move directly to results on electron density and tube content. Repeating the convention of K-1, we shall use dipole coordinates and an equatorial radius parameter, writing $4 R_E$ or $R_E = 4$ to indicate the geocentric equatorial distance 4 earth radii and, when appropriate, the field line with that distance to its equatorial crossing.

¹ On leave from Escola Polit cnica, Universidade de S o Paulo, Brasil.

EXPERIMENTAL RESULTS

Reference profile. As a reference for the results on the knee, we have calculated equatorial-density and total-tube-content profiles corresponding to the whistler shown on the upper record in Figure 1. This event was recorded at about 0150 LT during extremely quiet planetary magnetic conditions, when the equatorial distance to the knee is expected to be large (see K-1). Thus the many components in the whistler represent a broad range of field-line paths inside the knee. Figure 2 shows the calculated equatorial profile of electron density; Figure 3, the corresponding profile of total electron content in a tube of force versus dipole latitude at 1000 km. The latter profile is calculated for a tube with cross section of 1 cm² at 1000 km altitude and extending from 1000 km to the equatorial plane.

In Figures 2 and 3, and in many of the following figures, there are three types of data symbol, corresponding to three levels of precision in the measurements. The solid symbols represent highest precision; isolated open sym-

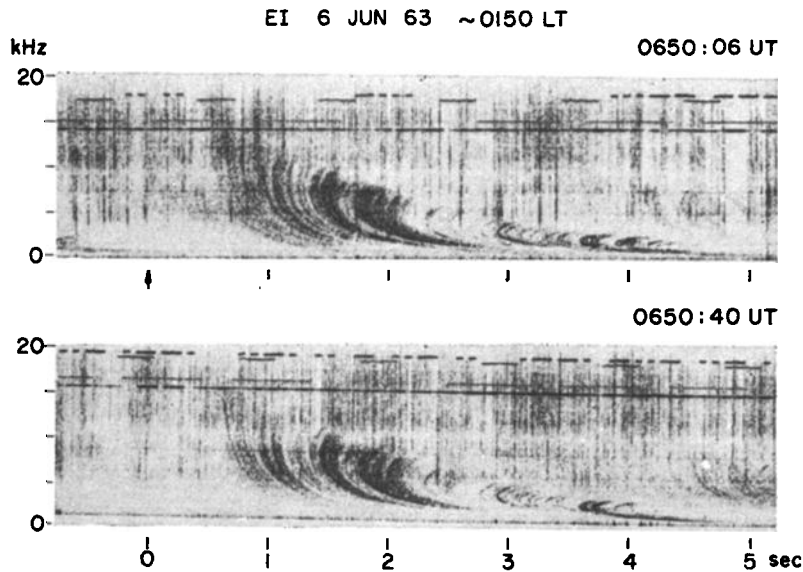


Fig. 1. Spectrograms of two whistlers recorded less than a minute apart at about 0150 LT on June 6, 1963, at Eights, Antarctica. Planetary magnetic conditions were extremely quiet at this time. Two events are shown to emphasize the repeatability of whistler properties on a scale of minutes. The horizontal lines at the top of the records represent transmissions from VLF stations.

bols, and next highest. In the lowest category are open symbols from which short lines extend to indicate the range of experimental error.

The equatorial profile of Figure 2, though intended as a reference, contains in itself some new information. Near $3 R_E$, the curve is relatively flat. The slope increases between 3.5 and $4 R_E$; from about 4 to $5.7 R_E$ the curve drops off roughly as R^{-4} . Most previous reports on the undisturbed profile have been based on averages from many events (see *Carpenter and Smith* [1964]). The profile has been found to fall between about R^{-3} and R^{-4} , but the averaging methods used may have tended to obscure certain changes in slope that can exist within a given profile.

The content profile of Figure 3 is also of special interest. It shows a relatively steady increase between 52° ($R_E \sim 3$) and 57° ($R_E \sim 4$), after which it remains roughly constant to the last measurement at 64° ($R_E \sim 6$). Were the content proportional to tube volume over the higher latitudes, it would increase by a factor of about 5 from 57° to 64° , following the trend shown from 52° to 57° .

Electron density near the knee on the night-side, 0100–0400 LT. Nightside data are of special interest because of the particularly large scale of the knee during the postmidnight hours. Several examples from the July–August period of 1963 are shown in Figure 4 in coordinates of electron density versus geocentric equatorial distance. Each example was found to be generally representative of conditions persisting for several hours or more. (The August 5 results are a composite of two roughly similar events recorded 3 hours apart.) For both events the magnetic condition was one of steady but moderate geomagnetic agitation, with the K_p index in the range 2–4. (Paper K-1 shows that, for such conditions, the knee is typically observed at about $4 R_E$ in the postmidnight hours.) The reference profile of Figure 2 is shown in Figure 4 as a continuous curve.

Two data points in a given multicomponent whistler may represent conditions on paths spaced several degrees apart in longitude. However, if the equatorial radius of the knee can be measured over periods long in comparison with the local-time spread in paths, it is frequently possible to interpret the results in

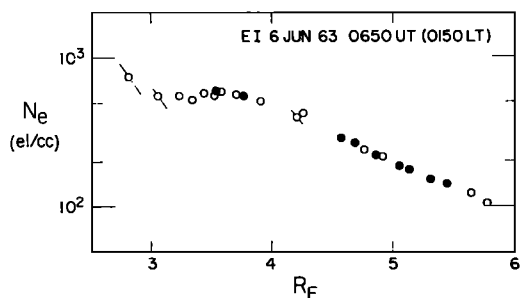


Fig. 2. Reference profile of equatorial electron density versus geocentric distance in earth radii, corresponding to the multicomponent whistler of Figure 1. Extremely quiet planetary magnetic conditions are represented. The various symbols indicate three levels of precision in the measurements, as described in the text.

terms of conditions on a given meridian. This is particularly true of post-midnight observations. For example, it was found that on August 4, 1963, the radius of the knee was unchanged for an hour before and an hour after the observation illustrated in Figure 4. (Such periods of unchanging radius are common, although on the average the radius decreases at night as described in K-1.) This implies that at 0850 UT, even with some longitude spread in the paths, the profile on any given meridian of longitude within several degrees of the meridian of Eights must have had approximately the form indicated by the data points in the figure.

From Figure 4 we draw the following conclusions, emphasizing that each set of points represents many similar observations on the same date.

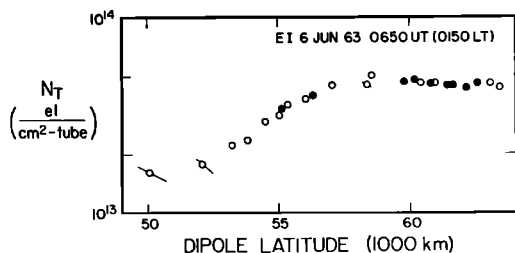


Fig. 3. Reference profile of total electron content in a tube of force (above 1 cm² at 1000 km) versus dipole latitude at 1000 km, corresponding to the whistler of Figure 1. Extremely quiet planetary magnetic conditions are represented.

1. At the knee, electron density drops by a factor between 30 and 100 within a distance less than about $0.15 R_E$. For the present, $0.15 R_E$ is the limit of our resolution. (The two data points at $\sim 4.5 R_E$ for July 7 represent an unusual case in which propagation was observed at an intermediate level between the top and bottom of the knee.)

2. The data points in the high-density region are distributed in a manner similar to that of the reference profile, but with values below the reference. This difference is tentatively attributed to the difference in the magnetic activity represented by the knee data and by the reference curve.

3. There is a general tendency for the data points to cluster at two well-defined levels (again with the exception of the July 7 case).

4. Data points in the low-density region are restricted to a fairly narrow region just outside the knee.

Spectrographic records of the July 8 event and of two other events recorded on July 8

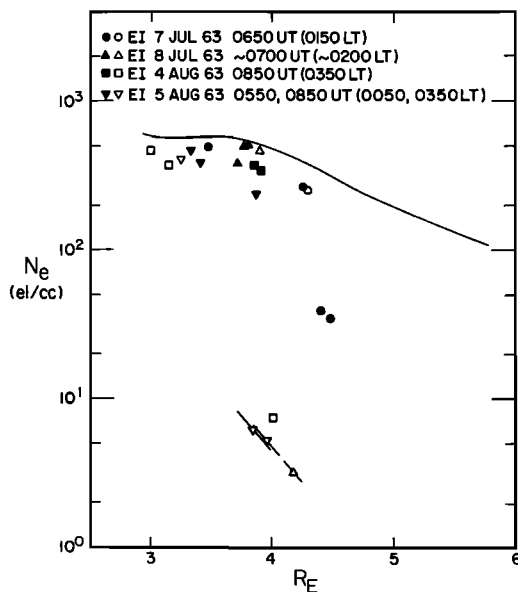


Fig. 4. Four profiles of equatorial electron density near the knee during the period 0100-0400 LT and for conditions of moderate, steady geomagnetic agitation ($K_p = 2-4$). The observations were made at Eights, Antarctica. The three types of symbol indicate three levels of precision, as described in the text. The solid curve is a representation of the reference profile of Figure 2.

EI 8 JUL 63 ~0200 LT

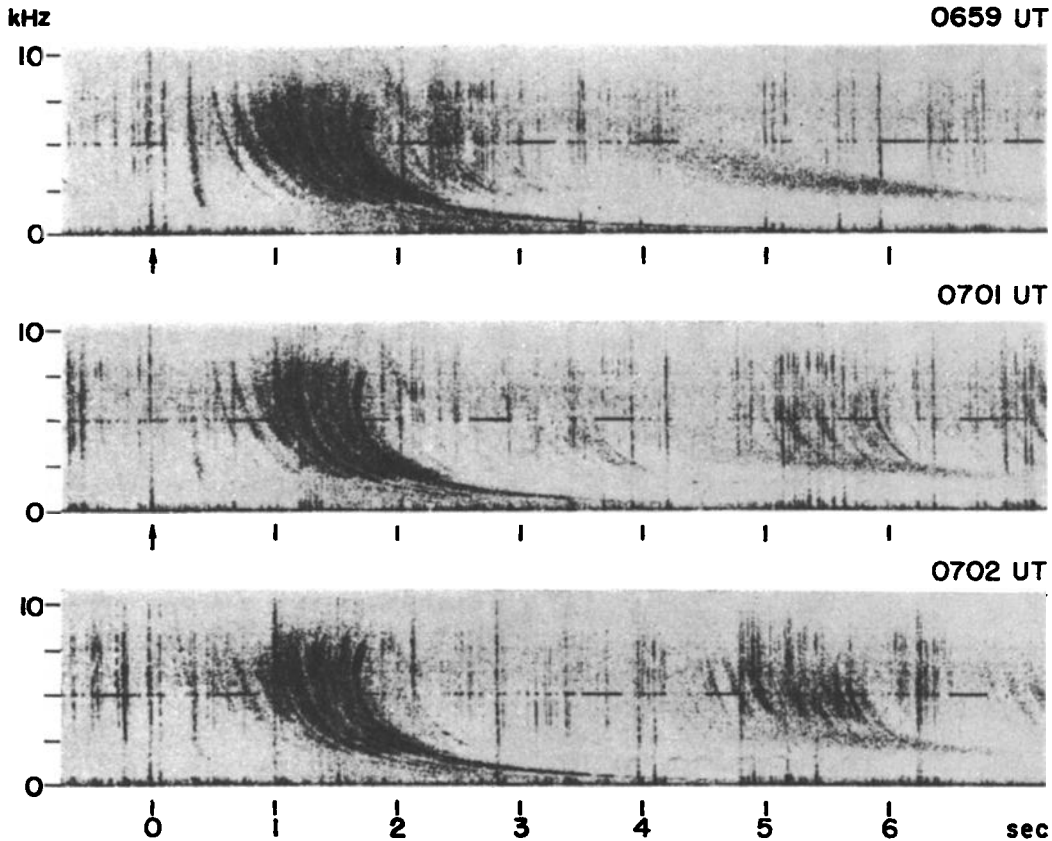


Fig. 5. Spectrograms of three whistlers observed within a period of about 3 minutes near 0200 LT on July 8, 1963, at Eights, Antarctica. The drastic knee effect is described in the text. The fixed-frequency signal injected near 5.0 kHz represents transmission from NBA at 18.0 kHz.

between 0659 and 0702 UT (about 0200 LT) are shown in Figure 5. In each of the three similar events, the main group of traces exhibits a pattern of descending nose frequency with increasing travel time at the nose. In the main group, nose frequencies range from above 10 to about 5.6 kHz, the travel time at the 5.6-kHz nose being about 1.8 seconds. The main body of traces is followed at a travel time of several seconds by a third-hop echo (somewhat obscured on the lower two records by other events). The most striking feature of the three whistlers is the single, somewhat diffuse trace propagating just outside the knee and showing a travel time of about 0.3 second. (Although the upper part of this trace is not well defined, partly owing to its near coincidence

with an impulsive sferic on the top record, examination by means of film techniques reveals a nose in the range 5.3–6.0 kHz.) The travel time of this component corresponds to a group velocity of approximately $c/2$, far greater than that customarily associated with whistlers.

Spectrograms of the event of August 4, 1963, are shown in Figure 6. Here the details are difficult to describe, owing to the presence of additional events in the background. At the right is a whistler with two closely spaced nose traces at a travel time of about 1.6 seconds. A strong, wide knee trace, limited in frequency range, appears with nose frequency of 6.3 kHz and travel time of 0.4 second (compare with Figure 5). At the left of the record is a whistler in which the observed components are

restricted to the region inside the knee. In this event, a trace with nose frequency at 12.6 kHz and nose travel time of about 0.6 second is well defined, as is a single trace with nose at 5.6 kHz, propagating near the inner edge of the knee.

Total electron content in tubes of force near the knee, 0100-0400 LT. The examples described above in terms of electron density in the equatorial plane are plotted in Figure 7 in terms of total electron content in tubes of force with cross section of 1 cm^2 at 1000 km and extending from 1000 km to the equatorial plane. Total content is of particular interest because, as was recently pointed out by Geisler and Bowhill [1965a], the calculated value of tube content is relatively insensitive to the choice of field-line model used in the computations.

Our conclusions about tube content are similar to those made about the equatorial profile. Within less than a degree at 1000 km, the total content above 1 cm^2 drops by a factor of about 20 (again excluding the July 7, event). Inside the knee, the data tend to follow the reference curve, but at a slightly lower level. The tendency of points to cluster at two well-defined levels is again clear.

The similarity between the equatorial and tube-content profiles suggests that the knee phenomenon is under strong geomagnetic control. Direct observations of a knee effect at points well removed from the equatorial plane have recently been made on Ogo 1 by Taylor *et al.* [1965] through mass-spectrometer measurements, and by Whipple and Troy [1965] using an ion trap.

Electron density near the knee in the after-

noon. Examples of equatorial profiles for the afternoon hours are shown in Figure 8. Again the magnetic condition represented is one of moderate and steady agitation. The scale of the knee, though apparently somewhat smaller than that of the nightside, remains large, involving a decrease by more than an order of magnitude. Again, there is a clear tendency for the data points to cluster near well-defined levels. The tenuous outer region is defined for a distance of several earth radii, well beyond the range of definition on the nightside (Figure 4). In the outer region, the profiles do not show a return to higher levels, but instead fall off steadily and with a smoothness (see August 4 and July 31) comparable to that of the reference profile for magnetically quiet conditions inside the knee (Figure 2). Near $7 R_E$, the electron density reaches 1 el/cm^3 , a factor of roughly 4 less than the ion densities reported for the region outside the magnetosphere boundary [Wolfe *et al.*, 1966].

The August 4 and July 31 profiles also exhibit a relatively large overlap, or double-valued condition, at the knee. Such an overlap, of the order of $0.3-0.4 R_E$ in extent, may be attributed to the combination of a longitude spread of paths in a multicomponent whistler and corresponding longitude variations in the equatorial radius of the knee. Many examples of large overlap occur in the late afternoon, and can be clearly identified with the rapid radial shift in the knee position described in K-1. Many others do not appear to be in that category, and we therefore suggest that a longitude ripple in the equatorial radius of the knee may sometimes occur on the dayside, with peak to peak amplitude as great as $0.4 R_E$.

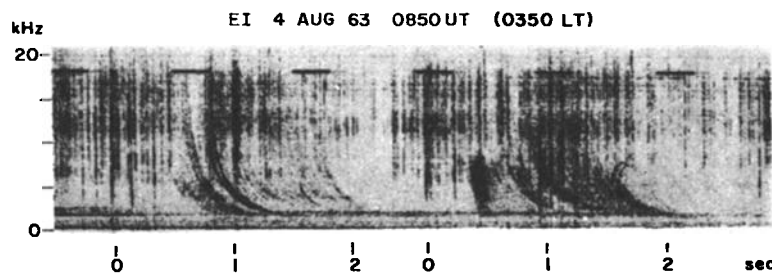


Fig. 6. Spectrograms of whistlers observed at about 0350 LT on August 4, 1963, at Eights, Antarctica. Two closely spaced whistlers are shown, with times of origin as indicated. Other faint whistlers appear in the background of the two principal events. The drastic knee effect is described in the text.

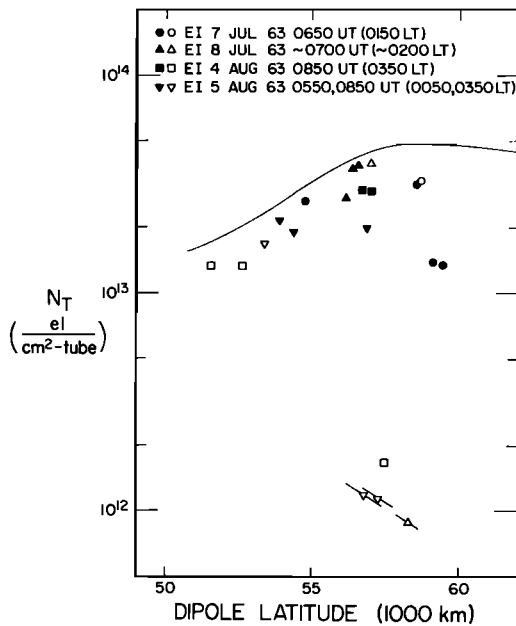


Fig. 7. Four profiles of total tube electron content versus dipole latitude at 1000 km during the period 0100-0400 LT. The magnetic condition is one of moderate, steady agitation ($K_p = 2-4$). The calculation is made for the volume extending from 1000 km to the equatorial plane and having a cross section of 1 cm^2 at 1000 km.

Because of the overlap effect, we make no detailed estimate of the slope at the knee for events recorded on the dayside. However, only an abrupt decrease, like that of the nightside, is easily reconciled with whistlers exhibiting large overlap in nose frequency at the knee. If the profile slopes relatively gradually, the spatial period of the postulated longitude ripples must be extended, the radial amplitude increased, and very large longitude spreading ($\sim 50^\circ$) of some whistlers assumed. These possibilities do not appear consistent with the data, but a detailed study of the longitude spread of whistler paths is needed to clarify this point properly.

Spectrograms of knee whistlers recorded in the afternoon are shown in Figure 9. The top record, for August 4, shows a large overlap effect and also indicates a smooth profile extending well outside the knee (see Figure 8). The overlap is evident in a comparison of the high-density trace (nose at ~ 6.0 kHz and nose

travel time ~ 1.6 seconds) and the first low-density trace (nose at ~ 9.5 kHz and nose travel time ~ 0.4 second). (The two traces at the right belong to other events). Details of the profile near $6-7 R_E$ were obtained through examination of the record illustrated and several hundred similar events recorded in a continuous run from 1700 to 2000 UT on August 4. The descending burst of noise near 1.5 kHz and 1.3 seconds actually describes closely the locus of nose frequency and nose travel time in this part of the spectrum.

The middle and bottom records in Figure 9 provide clear examples of the knee effect. These cases also exhibit some overlap in nose frequency at the knee, but the effects is not easily detected in this reproduction. Note, particularly on August 4 and July 28, the presence of noise triggered by traces propagating in the outer region. The record of July 28 also shows evidence of triggering just inside the knee, beginning at ~ 3.5 kHz, 1.5 seconds.

Total electron content in tubes of force near the knee in the afternoon. The total-content information corresponding to the profiles in Figure 8 is shown in Figure 10. The results are again similar to those shown on the equatorial

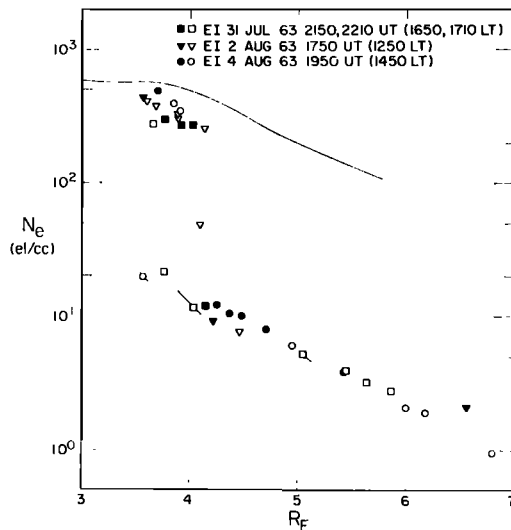


Fig. 8. Profiles of electron density versus geocentric distance in the equatorial plane, showing examples of the knee near $4 R_E$ during the afternoon. The apparent overlap at the knee is discussed in the text.

profile. The change in total content at the knee is slightly less than an order of magnitude.

Comparison of day and night profiles. Scatter plots including both day and nighttime data provide a useful summary of the results described above, as well as some specific information on day-night variations. To obtain the scatter plots of Figures 11 and 12, we present all the data from the previous plots, as well as additional data from the dayside for July 5, 1963, 2050 UT (1550 LT); July 28, 1963, 2150 UT (1650 LT); August 2, 1963, 1850 UT (1350 LT); August 5, 1963, 1550 UT (1050 LT); and July 7, 1963, 1250 UT (0750 LT). In the two figures, the open circles indicate daytime events, and the solid circles nighttime events from the period 0100 to about 0400 LT.

The data represent 11 independent recording periods, usually separated by 1 or more days and at minimum by 6 hours.

The data, though not conclusive in this matter, suggest that, in the region just inside the knee in the range $3.5-4 R_E$, the total tube content and density level vary only slightly from day to night. This condition may be related to previous whistler research showing the diurnal variation in magnetospheric electron density to be small [Iwai and Otsu, 1958; Rivault and Corcuff, 1960; Alcock, 1962]. Well inside the knee there appears to be a tendency for significantly lower values on the nightside, but the trend is not sufficiently well documented for further comment. Just outside the knee, the nightside values appear to be significantly lower

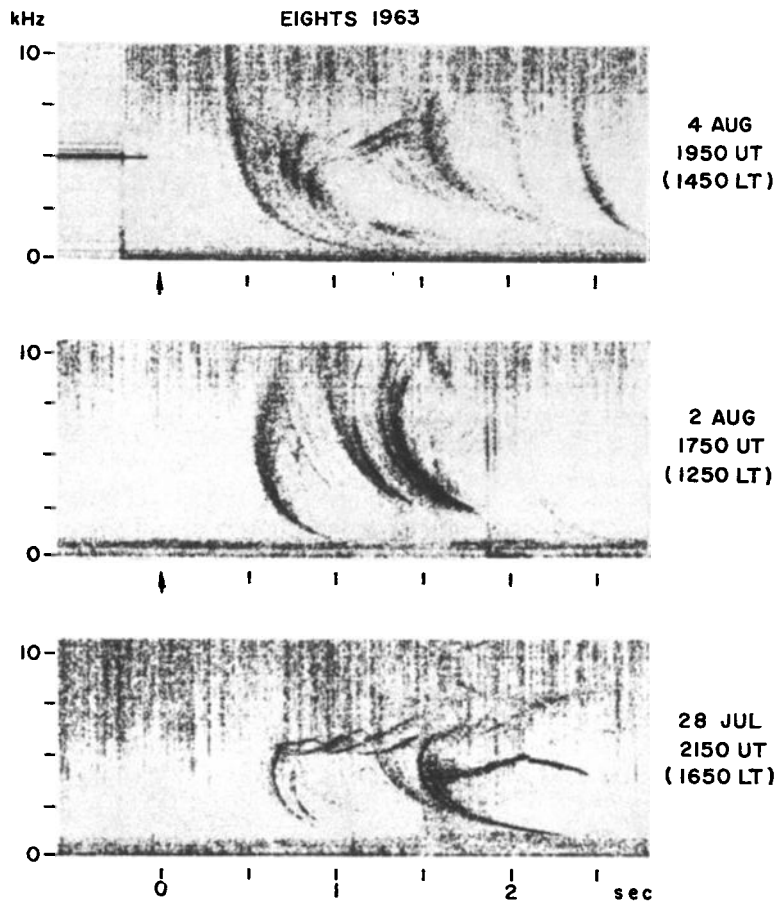


Fig. 9. Spectrograms of knee whistlers recorded in the afternoon at Eights, Antarctica. Several of the properties of these events are discussed in the text. The line at 5.0 kHz at the upper left is part of a system calibration.

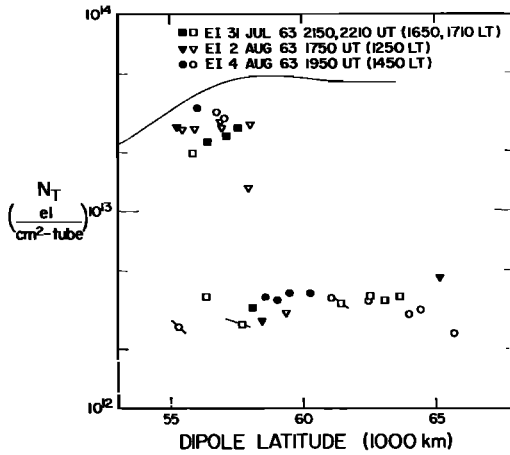


Fig. 10. Profiles of total tube electron content versus dipole latitude at 1000 km for afternoon observations when the knee is near $4 R_E$. The calculation is made for a volume extending from 1000 km to the equatorial plane and having a cross section of 1 cm^2 at 1000 km.

than the dayside values. (Recall that in Figures 11 and 12 the two solid points at $\sim 4.5 R_E$ ($\sim 59^\circ$) represent paths at some intermediate level on the knee profile.)

DISCUSSION

The problem of the field-line model of electron density. Information on magnetospheric electron density is obtained from whistlers through an integral relation between whistler travel time and the electron plasma frequency (see Carpenter and Smith [1964] or Helliwell [1965] and references cited therein). In performing an analysis it is customary to assume a model of the distribution of electrons along the field lines, and then from observational data obtain two parameters: the equatorial radius of the field-line whistler path, and the scale factor of the electron-density distribution.

Uncertainty in the field-line model of the distribution of ionization has relatively little effect on calculations of total tube content, a fact recently pointed out by Geisler and Bowhill [1965a]. In the case of equatorial profiles, lack of accurate knowledge of the model has relatively little effect on determinations of slope, while introducing an uncertainty of the order of $\pm 0.15 R_E$ in equatorial radius and an uncertainty by a factor of ± 2 in absolute value

of electron density [Carpenter and Smith, 1964]. Error on this scale is of minor importance in the detection of the presence and approximate position of the knee, but for purposes of investigating the details of the distribution of ionization near the knee special efforts to reduce error are necessary. A study has therefore been made with the object of finding models that would both accord with available experimental data and have theoretical support. Particular emphasis was placed on agreement with experimental data.

Results of the study of field-line models. For the high-density region inside the plasmopause, a diffusive-equilibrium distribution was found to be appropriate. For the outer region, a collisionless model behaving approximately as $N_e \propto R^{-4}$ was selected. The models are illustrated in Figure 13, where the coordinates are electron density, normalized to the value at the top of the path, versus path length along the $R_E = 4$ field line from the 1000-km level.

The d.e. model is based on a calculation by Angerami and Thomas [1964]. In working with this model we used the following parameters: ion abundances at 1000 km $[O^+] = 0.02$,

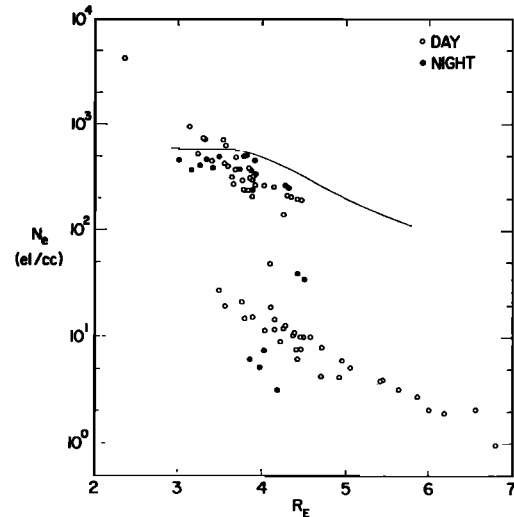


Fig. 11. Scatter plot including day and nighttime data on electron density in the equatorial plane versus geocentric distance in earth radii. The data from Figures 4 and 8 are included, as well as the additional data from the dayside described in the text. Conditions of moderate, steady geomagnetic agitation are represented ($K_p = 2-4$).

$[\text{He}^+] = 0.58$, $[\text{H}^+] = 0.40$; daytime temperature, 1600°K ; nighttime temperature, 1200°K . (Shawhan and Gurnett [1965] report the fractional abundance of H^+ at 1000 km to be about 0.80 on northern-hemisphere winter nights.) As the later discussion of error shows, these parameters are not critical for the determination of equatorial density or tube content using whistler data.

The collisionless model is based on the distribution deduced by *Eviatar et al.* [1964], who considered an ion-exosphere boundary separating a collisionless hydrogen plasma above and a Maxwellian hydrogen plasma below. In our calculations we took the ion-exosphere boundary to be at 1000 km and the temperature of the Maxwellian plasma to be 3200°K . The collisionless model is similar to the distribution $N_e \propto R^{-4}$, as Figure 13 indicates, and in what follows we shall use the description ' R^{-4} ' and 'collisionless' interchangeably. For simplicity, the calculations reported above for the low-density region were performed using the R^{-4} distribution.

The d.e. and R^{-4} models were chosen for the following reasons:

1. If we postulate that the knee represents a transition between an inner region where collisions are important in determining the field-line distribution, and an outer region where the field-line distribution is primarily exospheric in

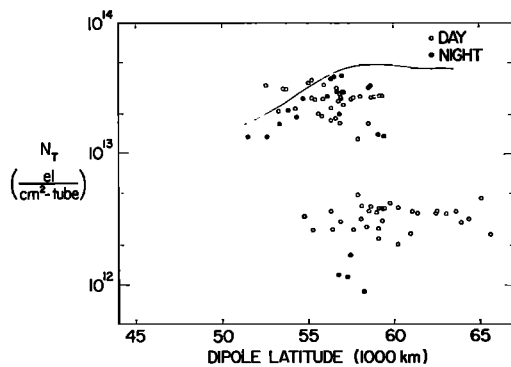


Fig. 12. Scatter plot of day and nighttime data on total tube content versus dipole latitude at 1000 km. The data are taken from Figures 7 and 10, and also include the additional data from the dayside described in the text. Conditions of moderate, steady geomagnetic agitation are represented ($K_p = 2-4$).

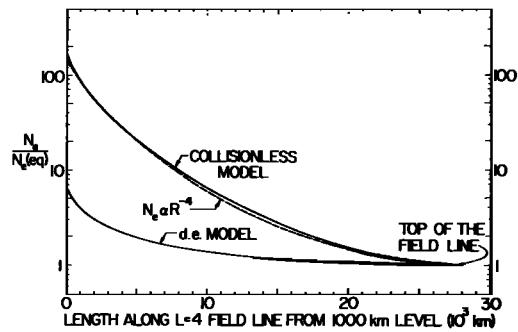


Fig. 13. Comparison of three field-line models of the distribution of ionization in the magnetosphere. The coordinates are electron density, normalized to the value at the equatorial plane, versus path length along the $R_E = 4$ dipole field line from the 1000-km level.

nature, then both models have theoretical support. With respect to the d.e. model, see *Dungey* [1955], *Johnson* [1960], *Mange* [1960], *Hanson and Ortenburger* [1961], *Bauer* [1962], *Angerami and Thomas* [1964]. For the collisionless model, see *Eviatar et al.* [1964].

2. The knee in magnetospheric ionization is more abrupt than the corresponding variation with latitude of ionospheric parameters such as ion density, electron temperature, and H^+ abundance. (A possible exception is the latitude variation of electron density near the F -layer peak at nighttime. See *Muldrew* [1965] and *Sharp* [1966].) This is particularly true in the daytime. Only a drastic model change at the knee, particularly with respect to slope at great heights, is compatible with conditions both high and low along the field lines. For relevant information on electron density in the ionosphere, see *DRTE Alosyn* [1965] report, or *Thomas and Sader* [1964]. On H^+ abundance, see *Shawhan and Gurnett* [1965] and *Barrington et al.* [1965].

3. Comparison of *Alouette 1* measurements of electron density at 1000 km [*DRTE Alosyn*, 1965] and 1000-km electron densities calculated from whistlers indicates relatively good agreement when the d.e. and R^{-4} models are used. Examples of the agreement are shown in Figures 14 and 15 in coordinates of electron density at 1000 km versus L value. Figure 14 shows the data from the reference whistler (Figure 1) for magnetically quiet nighttime conditions, and

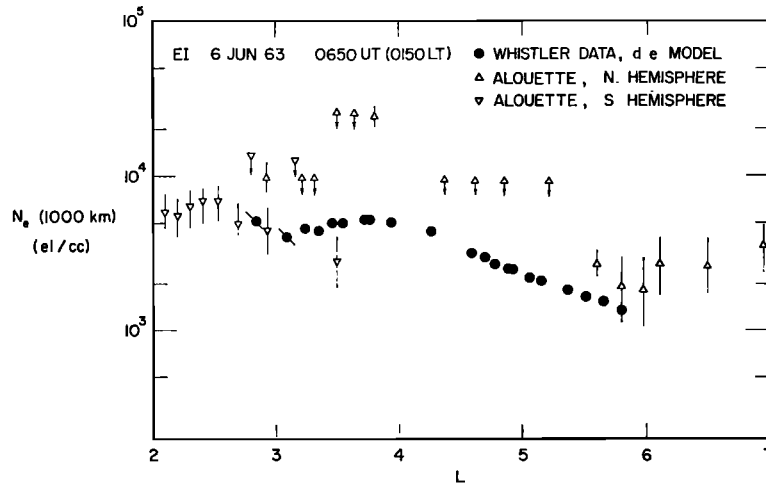


Fig. 14. Comparison of Alouette observations and 1000-km electron densities deduced using whistler data and the diffusive-equilibrium field-line model. The L values are those reported in the *DRTE Aloyn* [1965] report. The whistler data are from the reference whistler illustrated in Figure 1.

Figure 15 data from a knee whistler (knee at about $4 R_E$) in the afternoon. In both figures, the Alouette data represent tracks near the meridian of Eights Station and times within roughly an hour of the whistler observations. Figure 14 suggests that good agreement at 1000 km may be obtained using the d.e. model inside the knee (a properly detailed study reconciling whistlers and Alouette data has not yet been made). Figure 15 shows agreement in slope but a discrepancy in level. The discrepancy may be due to one of several factors not taken into account in the field-line models, including the possibility of departures from diffusive equilibrium associated with the slow diffusion process described by *Geisler and Bowhill* [1965b], and also the possibility of a relatively high concentration of oxygen ions at 1000 km. The important point is that, if the d.e. model were applied on both sides of the knee, the whistler calculations would show an abrupt decrease near $L = 4$ by a factor of about 7, in distinct contrast to the Alouette observations.

4. The change in high-altitude slope between the d.e. and R^{-4} models is compatible with a special property of whistlers, an overlap in nose frequency at the knee, in which the nose frequency of a component propagating outside the plasmopause is higher than the lowest nose frequency inside. This is not the large overlap ob-

served on the dayside, but rather a smaller, 10–15% effect, found between 0100 and 0400 LT, in which longitude variations in the boundary radius do not appear to be a governing factor. The effect is shown schematically in Figure 16a, where horizontal lines are drawn at the relevant nose frequencies. If the d.e. model is applied on both sides of the knee, the deduced profile has the double-valued appearance shown in Figure 16(b). When calculations are made using the d.e. model inside the $N_e \propto R^{-4}$ outside, the low-density point is shifted by about $0.2 R_E$ in the manner indicated. At the same time, the calculated value of equatorial electron density is decreased by a factor of about 3.

Having now outlined the arguments for the choice of models, we present estimates of error in the profiles. Because of the low electron densities near $7 R_E$ on the afternoon profile, special attention will be devoted to error in this region.

Error in the profiles. Estimates of uncertainty in the profiles shown earlier are presented in Figures 17 and 18. The dashed line is intended to indicate approximate position with respect to the knee. For all parts of the equatorial profile (Figure 17), the largest uncertainty concerns the choice of field-line model used in the calculations. Inside the knee, the error range is determined by allowing wide variations in the

temperature and fractional abundances of ions used in the d.e. model, and also in the effect of the regular ionosphere. Outside the knee, additional considerations are brought to bear, as described below. In the case of the content profiles (Figure 18), the largest uncertainty lies in the effect of the ionosphere below 1000 km. Again, the error was estimated by allowing wide variations in the model parameters and in the ionospheric effect. In both figures there is a trend toward increasing uncertainty with increasing equatorial radius, but in general the error is small with respect to the scale of the knee, remaining at or below a factor of ± 2 for the equatorial densities and ± 1.5 for the tube content.

Discussion of the estimate of 1 el/cm^3 at $7 R_E$. A number of factors that may affect the calculations of equatorial electron density at $7 R_E$ include: (1) inaccuracy in the field-line electron-density model used in the calculations; (2) distortion of the field lines; (3) temperature effects on the frequency-time properties of whistlers; (4) corrections to the refractive index associated with unusually low ratios of electron-plasma to electron-cyclotron frequency. In regard to the model uncertainty, only a distribution with a very gradual slope near the top of the path, such as the d.e. model, could be used to increase significantly the estimate of electron den-

sity, to a value of, say, 3 or 4 el/cm^3 near $7 R_E$. However, as previously explained, the d.e. model is not compatible with conditions at both low and great heights outside the plasmapause. Less extreme variations around the R^{-4} model, as well as ionospheric variations, must be considered, but in these cases the range of calculated values falls within a factor of about ± 1.5 of the R^{-4} results.

The result of assuming a dipole field in the presence of a compressed outer geometry is to place points on the approximately correct equatorial profile, but at geocentric distances that are too low (by about $1 R_E$ near $7 R_E$). This is because the two factors, changed equatorial crossing of the field line and changed path length, tend to have opposing effects. In a compressed field, a field-line path crossing the equator at $8 R_E$ produces a whistler of nose frequency assigned to about $7 R_E$ in the dipole model (see, in this connection, Mead [1964]). However, when the electron-density calculation is made, the path length assigned in the calculations is too short, being the path length for the dipole field line passing through $7 R_E$, rather than the distorted, longer line through $8 R_E$. The calculated value of equatorial electron density is then too high (for $8 R_E$), but it is plotted for $7 R_E$, and thus tends to fall near the correct profile. There are additional matters of detail to

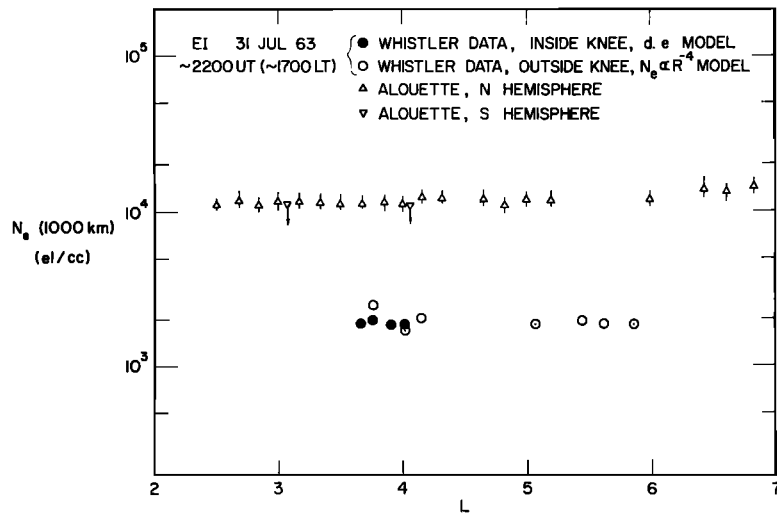


Fig. 15. Comparison of 1000-km electron densities deduced from a knee whistler observed in the afternoon and Alouette data recorded within about 1 hour of the whistler observation. See text for details, including an explanation of the overlap in solid and open circles.

be considered in this explanation, but they must be deferred for a more thorough treatment.

The refractive index for whistler propagation is modified when the thermal motions of the electrons are taken into account. Once again, however, there are effects that tend to cancel one another. The thermal motion of the particles tends to lower the effective gyrofrequency of a significant number of the particles and thus to slightly depress the nose frequency of the whistler. However, the thermal effects also tend to increase the travel time of the whistler [Guthart, 1965; Scarf, 1962]. The result is that a datum point on the equatorial profile is plotted slightly too high in equatorial radius but too low in density. Again, the profile is approximately correct. This effect is probably somewhat smaller than the effect introduced by the distortion of the earth's field.

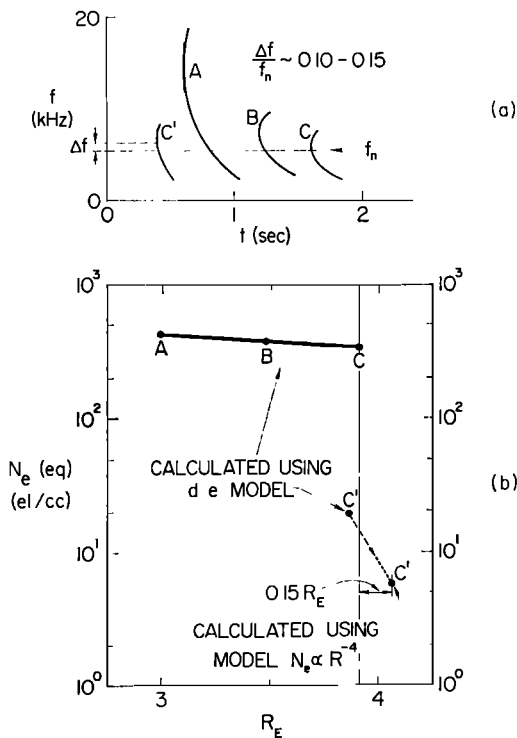


Fig. 16. (a) Idealized frequency-versus-time properties of a nighttime whistler exhibiting overlap in nose frequency at the knee. (b) Calculations of equatorial electron density based on the four components in (a). The effect of using two different field-line models in making the calculations for trace C' is shown.

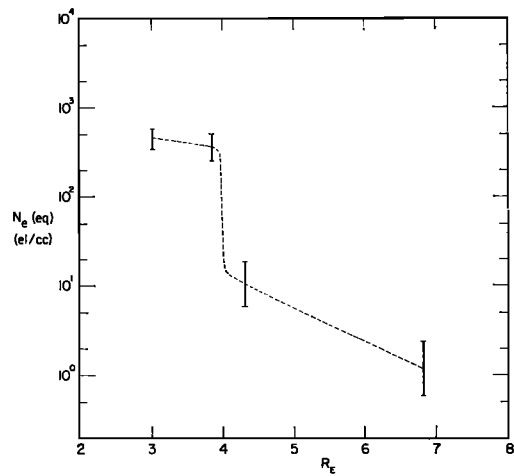


Fig. 17. Estimated uncertainty in the equatorial values of electron density calculated from whistler data. The dashed line is intended only to indicate the approximate position of the knee at about 4 R_E . The principal contribution to the uncertainty is not measurement error but uncertainty in the field-line model of the distribution of ionization used in the calculations.

The expression for the refractive index at whistler frequencies must be modified when the ratio of electron plasma frequency to cyclotron frequency becomes sufficiently low. That is, the expression

$$n^2 = 1 + [f_p^2 / f(f_H - f)]$$

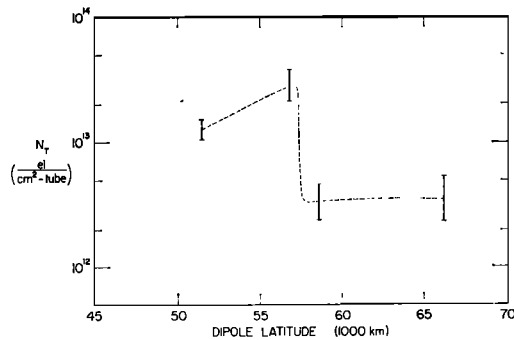


Fig. 18. Estimate of uncertainty in the values of total tube electron content calculated from whistler data. The principal contribution to the uncertainty is not from measurement error but from uncertainty in the contribution of the regular ionosphere below 1000 km to the observed effects.

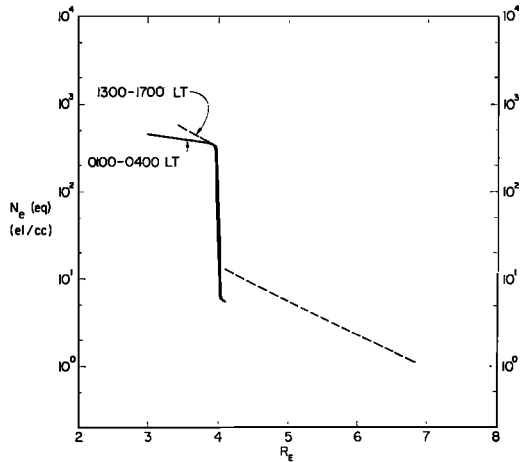


Fig. 19. Estimated average equatorial profiles of electron density for the periods 0100-0400 LT and 1300-1700 LT. The profiles are based on the data described earlier in the paper. The dashed curve is interrupted at the knee to take account of the overlap ambiguity described in the text. The geocentric range covered by the profiles is intended to show the regions for which a significant amount of data was examined. The magnetic condition represented is one of steady, moderate agitation, with K_p in the range 2-4.

for the square of the phase refractive index must be used in place of the approximation

$$n^2 \cong f_p^2 / (f_H - f)$$

This effect becomes of importance in the region outside the knee, where the ratio f_p/f_H may approach unity. Some calculations using the full expression showed that the nose frequency is affected only negligibly but that in a tenuous medium the calculated whistler travel time for a given electron density is somewhat increased. Thus, in the region outside the knee, the profiles in Figure 8 represent an estimate that may be high by a factor of 20 to 30%. Again, however, the affect is relatively small.

In view of the foregoing, our conservative estimate of uncertainty in the dayside profile well outside the knee is a factor of ± 2 (see Figure 17). A correspondingly conservative estimate for the content profile (Figure 18) is a factor of ± 1.5 .

CONCLUSIONS

The results on equatorial electron density and on tube electron content are summarized in

Figures 19 and 20. Recall that the observations were made at Eights Station in July and August of 1963, during conditions of moderate but steady geomagnetic agitation ($K_p = 2-4$). In both figures, the continuous curve represents the nighttime period 0100-0400 LT and the dashed line represents afternoon observations. The dashed line is interrupted at the knee in order to take account of the overlap ambiguity described above.

In performing the calculations we found it appropriate to apply a model of hydrostatic equilibrium for the distribution of electrons along the field lines inside the plasmapause, and a collisionless model ($\sim N_e \propto R^{-4}$), adapted from the report of *Eviatar et al.* [1964], for the region outside. In choosing these models we appealed to both theoretical and experimental sources, making a particular effort to reconcile the models with satellite measurements along the topside ionosphere and with various relevant properties of whistlers. The experimental data provide particularly strong evidence that the slope of the field-line distribution near the top of the path varies significantly from one side of the knee to the other.

In paper K-1 a remarkable repeatability was found in the diurnal variation of knee position for conditions of moderate and steady geomagnetic agitation. From the present paper it is

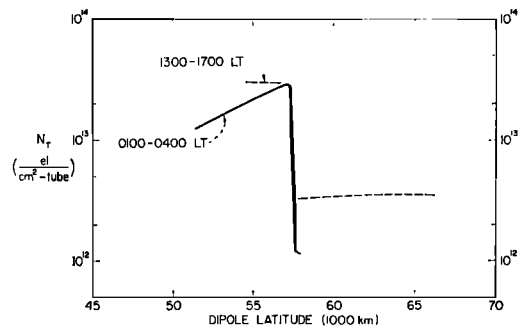


Fig. 20. Estimated average behavior of the profiles of total electron content versus dipole latitude at 1000 km during the periods 0100-0400 LT and 1300-1700 LT. The calculation is for a tube volume extending from 1000 km to the equatorial plane, with cross section of 1 cm^2 at 1000 km. The curves are restricted to the region for which a significant amount of data was examined. The magnetic condition represented is one of steady moderate agitation, with K_p in the range 2-4.

clear that, at least for 0100–0400 and 1300–1700 LT, there is a corresponding repeatability in the density and content profiles. During the postmidnight hours and, quite possibly, in the afternoon, the bulk of the equatorial density decrease takes place within $0.15 R_E$ (the present limit of our resolution). Both the scale of the knee and the absolute levels of density are roughly the same for postmidnight and for day-side observations. Because of the persistence of the knee both in equatorial radius (see K-1) and in approximate shape over periods of the order of 10 hours, we conclude that the profile illustrated in Figure 19 represents a kind of equilibrium state in the magnetosphere.

The reference profile of Figure 2 suggests that for quiet conditions, when the equatorial distance to the knee is large, the slope of the nighttime equatorial profile may increase from a flat characteristic near $3 R_E$ to an $\sim R^{-4}$ variation beyond $4 R_E$. The corresponding reference for tube content (Figure 3) shows that, beyond 57° ($R_E \sim 4$), the content may remain at a constant level over a range corresponding to $2 R_E$ at the equator.

The knee profiles of Figures 19 and 20 provide some evidence on the diurnal variation of protonospheric density and content. On the equatorial profile, the variation appears small just inside the knee but may increase with decreasing distance. Outside the knee, the night-day variation is clearly evident, although the nighttime data are restricted to the region near the bottom of the knee. In the presence of an upward flux of particles on the dayside, we would expect the night-day variation in tube content to be most pronounced at latitudes where the nighttime content is relatively low. The observed variation (Figure 20) is indeed pronounced outside the knee, whereas the high-content region near 57° remains relatively unaffected. The variation may again be large well inside the knee, but further study of this point is required. (For the present, we exclude discussion of the transition from day to night. Its complexity is compounded by the peculiar variation in the knee position between about 1700 and 0000 LT; see K-1.)

The shape of the content profile in Figure 20 allows us to conclude that much of the temporal variation in the position of the knee cannot be attributed to diffusion of ionization along

field lines. As is indicated in paper K-1, the equatorial distance to the knee may change significantly in a period of the order of an hour. If, for example, an inward movement were attributed strictly to a downward flux depleting certain tubes of ionization, the flux would have to be at least of the order of 10^{10} el/cm² sec and also be highly restricted in its distribution over latitude. Thus it seems evident that, although the process giving rise to the knee may profoundly influence the nighttime ionosphere, the shape of the knee and its movements are not directly controlled by the coupling between the protonosphere and ionosphere.

The occasional presence of a large overlap in nose frequency at the knee leads us to postulate the existence of longitude ripples in the equatorial radius of the knee on the dayside. If, as is possible, these ripples are the manifestation of occasional wide longitude spreading in whistler paths from a single source, the overlap may be due simply to the type of regular diurnal variation in the knee position described in paper K-1.

Afternoon profiles have been found to be extremely smooth over a range of several earth radii outside the knee. On such profiles, electron density drops below about 1 el/cm³ near $7 R_E$. This value is a factor of about 4 lower than the ion densities reported for the region outside the magnetosphere boundary [Wolfe *et al.*, 1966], thus implying the presence of some kind of boundary knee near the magnetopause, at which the density returns to a higher level.

Acknowledgments. We wish to thank G. Nelms and his colleagues of the Defence Research Telecommunications Establishment for their cooperation in making available topside sounder data from Alouette 1.

We are particularly grateful to J. Katsufakis of this laboratory for his prominent role in the development of the Stanford recording program in the Antarctic. We also thank Professor R. A. Helliwell for many conversations and suggestions during the course of the research. We have benefited from discussions with F. L. Scarf.

This research was supported in part by the National Science Foundation Office of Antarctic Programs under grant NSF GA-144, the Atmospheric Sciences Section under grant NSF GP-1191, and the Office of Computer Sciences in the Mathematical Division under grant NSF GP-948, and in part by the U. S. Air Force under contract AFOSR 783-65, monitored by the Air Force

Office of Scientific Research of the Office of Aerospace Research.

REFERENCES

- Allcock, G. McK., IGY whistler results, *Monograph on Radio Noise of Terrestrial Origin*, edited by F. Horner, p. 116, American Elsevier, New York, 1962.
- Angerami, J. J., and J. O. Thomas, Studies of planetary atmospheres, 1, The distribution of electrons and ions in the earth's exosphere, *J. Geophys. Res.*, **69**(21), 4537-4560, 1964.
- Barrington, R. E., J. S. Belrose, and G. L. Nelms, Ion composition and temperatures at 1000 km as deduced from simultaneous observations of a VLF plasma resonance and topside sounding data from the Alouette 1 satellite, *J. Geophys. Res.*, **70**(7), 1647-1664, 1965.
- Bauer, S. J., On the structure of the topside ionosphere, *J. Atmospheric Sci.*, **19**, 276-278, 1962.
- Carpenter, D. L., Whistler studies of the plasma-pause in the magnetosphere, 1, Temporal variations in the position of the knee and some evidence on plasma motions near the knee, *J. Geophys. Res.*, **71**(3), 1966.
- Carpenter, D. L., and R. L. Smith, Whistler measurements of electron density in the magnetosphere, *Rev. Geophys.*, **2**(3), 415-444, 1964.
- DRTE Alosyn: *Alouette 1 Ionospheric Data*, Defence Research Telecommunications Establishment, Ottawa, Ontario, Canada, 1965.
- Dungey, J. W., Electrodynamics of the outer atmosphere, *The Physics of the Ionosphere*, p. 299, The Physical Society, London, 1955.
- Eviatar, A., A. M. Lenchek, and S. F. Singer, Distribution of density in an ion-exosphere of a nonrotating planet, *Phys. Fluids*, **7**, 1775-1779, November 1964.
- Geisler, J. E., and S. A. Bowhill, The relation between the dispersion of a whistler and the electron temperature in the protonosphere, *J. Atmospheric Terrest. Phys.*, **27**, 122-125, 1965a.
- Geisler, J. E., and S. A. Bowhill, An investigation of ionosphere-protonosphere coupling, *Univ. Illinois Aeronomy Rept. 5*, January 1, 1965b.
- Guthart, H., Nose whistler dispersion as a measure of magnetospheric electron temperature, *Radio Sci.*, November 1965.
- Hanson, W. B., and I. B. Ortenburger, The coupling between the protonosphere and the normal F region, *J. Geophys. Res.*, **66**, 1425-1435, 1961.
- Helliwell, R. A., *Whistlers and Related Ionospheric Phenomena*, Stanford University Press, Stanford, California, 1965.
- Iwai, A., and J. Otsu, On the characteristic phenomena for short whistlers observed at Toyokawa in winter, *Proc. Res. Inst. Atmosphere, Nagoya Univ.*, **5**, 53-63, 1958.
- Johnson, F. S., The ion distribution above the F_2 maximum, *J. Geophys. Res.*, **65**(2), 577-584, 1960.
- Mange, P., The distribution of minor ions in electrostatic equilibrium in the high atmosphere, *J. Geophys. Res.*, **65**(11), 3833-3834, 1960.
- Mead, G. D., Deformation of the geomagnetic field by the solar wind, *J. Geophys. Res.*, **69**(7), 1181-1195, 1964.
- Muldrew, D. B., F-layer ionization troughs deduced from Alouette data, *J. Geophys. Res.*, **70**(11), 2635-2650, 1965.
- Rivault, R., and Y. Corcuff, Recherche du point conjugué magnétique de Poitiers—variation nocturne de la dispersion des sifflements, *Ann. Geophys.*, **16**(4), 530-554, 1960.
- Scarf, F. L., Landau damping and the attenuation of whistlers, *Phys. Fluids*, **5**(1), 6-13, 1962.
- Sharp, G. W., A mid-latitude trough in the night ionosphere, *J. Geophys. Res.*, **71**(5), 1966.
- Shawhan, S. D., and D. A. Gurnett, *Method of Determining $\alpha = n(H^+)/n_e$ and the Ion Temperature from Measurements of Proton Whistlers*, Department of Physics and Astronomy, University of Iowa, Iowa City, April 1965.
- Taylor, H. A., H. C. Brinton, and C. R. Smith, Preliminary results from measurements of hydrogen and helium ions below 50,000 km, paper presented at American Geophysical Union Meeting, Washington, D. C., April 19-22, 1965.
- Thomas, J. O., and A. Y. Sader, Electron density at the Alouette orbit, *J. Geophys. Res.*, **69**(21), 4561-4581, 1964.
- Whipple, E. C., and B. E. Troy, Preliminary ion data from the planar ion-electron trap on Ogo 1, paper presented at American Geophysical Union Meeting, Washington, D. C., April 19-22, 1965.
- Wolfe, J. A., R. W. Silva, and M. A. Myers, Preliminary results from the Ames Research Center plasma probe observations of the solar wind-geomagnetic field interaction region on Imp 2 and Ogo 1, *Space Res.*, **6**, 1966.

(Manuscript received September 24, 1965;
presentation revised November 1, 1965.)